Review

A Simple Phthalocyanine-Peptide Conjugate as Targeting Photosensitizer and Its Broad Applications in Health

Zheng Chen [1], Jincan Chen [2], Dafeng Liu [3], Jingyi Chen [1], Linlin Li [1], Dan Chen [1], Naisheng Chen [1], Jinling Huang [1], Zhuo Chen [2], Peng Xu [4], Longguang Jiang [1], Cai Yuan [4,*], Yunbin Jiang [5,*] and Mingdong Huang [1,*]

[1] National & Local Joint Biomedical Engineering Research Center on Photodynamic Technologies, College of Chemistry, Fuzhou University, Fuzhou 350108, China
[2] State Key Laboratory of Structural Chemistry, Fujian Institute of Research on the Structure of Matter, Chinese Academy of Sciences, Fujian College, University of Chinese Academy of Sciences, Fuzhou 350002, China
[3] College of Chemistry and Chemical Engineering, Xiamen University, Xiamen 361005, China
[4] College of Biological Science and Engineering, Fuzhou University, Fuzhou 350108, China
[5] School of Biological Science and Biotechnology, Minnan Normal University, Zhangzhou 363000, China
* Correspondence: cyuan@fzu.edu.cn (C.Y.); jyb1972@mnnu.edu.cn (Y.J.); HMD_lab@fzu.edu.cn (M.H.)
Received: 28 August 2024; Revised: 9 October 2024; Accepted: 17 October 2024; Published: 25 October 2024

Abstract: Photodynamic therapy is a novel clinical treatment for malignant tumors, and has recently been extended to anti-bacteria and anti-virus applications. Phthalocyanine photosensitizers possess good photosensitization properties, but their high hydrophobicity and lack of targeting capabilities limit their application. By conjugating a pentalysine peptidyl moiety to hydrophobic phthalocyanine, a novel photosensitizer ($ZnPc(Lys)_5$) was synthesized. This review systematically summarizes the design, development, safety and characterization of $ZnPc(Lys)_5$, and describes its applications and mechanisms in anti-tumor, anti-bacterial and anti-viral areas, as well as exploring its prospects for applications beyond photodynamic therapy. This review demonstrates that the peptide conjugation is an effective strategy for enhancing water solubility and broadens the applications of phthalocyanine-type photosensitizers. Furthermore, the importance of dynamic balance between the monomeric and aggregate conformations of phthalocyanine underlying its photodynamic effect is highlighted, providing a fresh perspective for the design and application of photosensitizers.

Keywords: photosensitizer; photodynamic therapy; targeting; anti-tumor; antibacterial; monomer-aggregate dynamics

1. Introduction

1.1. Photodynamic Therapy

At the beginning of the 20th century, Oskar Raab, under the mentorship of Hermann von Tappeiner, discovered the phenomenon of light-induced damage to microorganisms [1]. This laid the foundation for the development of photodynamic therapy (PDT), a treatment modality currently applied to various diseases, including cancer [2,3], ocular diseases [4], and skin conditions [5,6].

PDT involves three main steps [7]: (1) Cellular uptake of the photosensitizer; (2) Photoactivation of the photosensitizer at an appropriate wavelength, leading to the generation of reactive oxygen species (ROS); (3) Reaction of ROS with nearby molecular targets, inducing cellular damage and death. The efficacy of PDT is highly influenced by the properties of the photosensitizer. Notable examples include porphyrins, phthalocyanines, and their derivatives and modifications [2,8,9].

1.2. Development of Photosensitizers

Based on the three essential elements of PDT (photosensitizer, light, and oxygen) and the treatment process, ideal photosensitizers should have the following characteristics [2,8]: (1) Strong photosensitizing ability, characterized by a high photodynamic quantum yield; (2) Longer excitation wavelengths, allowing for deeper tissue penetration; (3) High selectivity for target tissues with no toxic side effects on normal tissues; (4) High

purity, with a well-defined structure without too many isomers and should be stable; (5) Rapid elimination of excess drug from the body after treatment; (6) A certain degree of water solubility under physiological conditions.

Photosensitizers can be broadly classified into the following three generations:

- The first-generation photosensitizers

The representative first-generation photosensitizers include Hematoporphyrin derivative (HpD), Dihaematoporphyrin ether (DHE), and Photofrin. They all have numerous drawbacks, such as complex compositions; low selectivity for tumor tissues, requiring larger doses of medication for treatment; significant skin phototoxicity, which requires the patients to stay in a dark room to avoid prolonged exposure to light after photodynamic treatment. All these factors have severely limited their scope of application.

- The second-generation photosensitizers

The second-generation photosensitizers, which were developed after the 1980s, are primarily porphyrin compounds with well-defined compositions and structures. They partially overcame the shortcomings of the first-generation photosensitizers, such as complex compositions and poor tissue permeability, with higher photosensitizing activity, redshifted absorption wavelengths, metabolic rates in vivo, and tissue selectivity [10,11].

- The third-generation photosensitizers

The third-generation photosensitizers are currently under development. They are primarily produced by the introduction of functional modules with biological properties or molecular recognition capabilities onto second-generation photosensitizers. These functional modules include proteins, liposomes, corresponding antibodies and ligands for antigens or receptors expressed in tumor tissues [9]. Besides enhancing the selectivity of photosensitizers for target tissues, these functional modules also improve the water solubility of photosensitizers under physiological conditions, thereby expanding their application scope.

1.3. Phthalocyanine-Type Photosensitizers

Phthalocyanine is one of the important members of photosensitizers characterized by an 18-π electron conjugated system and a central cavity approximately 0.27 nm in diameter. When hydrogen atoms in the cavity are replaced with metal ions, stable metal phthalocyanines form. These complexes exhibit excellent photosensitizing properties, characterized by high molar extinction coefficients, high singlet oxygen quantum yields, and maximum absorption wavelengths (670–680 nm) located in the near-infrared region. This long wavelength allows deeper penetration through human tissues [12]. However, phthalocyanines are highly hydrophobic, and tend to aggregate through π-π interactions, severely compromising their photodynamic efficacy [13]. Structural modification of phthalocyanines is one approach to address aggregation issues. A novel phthalocyanine photosensitizer was previously developed by some of the authors in the manuscript [14,15]. This photosensitizer contains two sulfonic groups which enhance water solubility, and is currently in Phase II clinical trials for cancer treatment.

1.4. Peptides as Functional Modules

In this study, peptide conjugation was performed to reduce the hydrophobicity of phthalocyanines. Peptides offer several unique advantages as targeting moieties including: (1) Adjustable hydrophilic/hydrophobic balance of the conjugate through appropriate peptide selection; (2) Targeted binding to tissue receptors by specific peptides; (3) Creates peptide-photosensitizer conjugates with molecular weights compared to proteins, facilitating cellular uptake via endocytosis [16]; (4) Defined composition of the peptide-photosensitizer conjugates. Commonly used peptides include receptor-specific peptides [17] and polylysine [18].

2. Development, Synthesis, and Characterization of ZnPc(Lys)$_5$

2.1. Design of ZnPc(Lys)$_5$, Lyscyanine

Our team successfully synthesized a β-monocarboxylate-substituted phthalocyanine zinc (ZnPc(COOH) or CPZ) with high purity (95%), which allows further chemical conjugation to other groups or derivatization [19]. The results demonstrated that the water solubility and targeting capability of CPZ were improved following the conjugation with various functional modules, including different lengths of polylysine [13,20,21], hormone peptides [22], protein ligands targeting specific receptors [23], and small molecules [24].

This review discusses the conjugation of CPZ with a simple peptide (pentalysine), to form the zinc phthalocyanine-pentalysine conjugate (ZnPc(Lys)$_5$, named Lyscyanine). This conjugate exhibited good water

solubility and excellent photodynamic effects [13]. A series of zinc phthalocyanine-polylysine conjugates with varying number of amino acid lysine ($ZnPc(Lys)_n$, n = 1, 3, 5, 7, 9) were synthesized to explore the optimal number of lysine. In photodynamic anti-tumor experiments, these conjugates exhibited low skin phototoxicity (IC_{50} > 100 μM), in the absence of light, but good phototoxicity against gastric adenocarcinoma cells (BGC823), while $ZnPc(Lys)_7$ (IC_{50} = 1.9 μM) and $ZnPc(Lys)_5$ (IC_{50} = 5.0 μM) demonstrated similarly high photocytotoxicity [21]. In photodynamic antibacterial experiments against *Escherichia coli*, $ZnPc(Lys)_5$, despite having slightly lower uptake than $ZnPc(Lys)_7$, exhibited the highest antibacterial activity with a minimum inhibitory concentration of 25.3 μM, half that of $ZnPc(Lys)_7$[25]. Thus, $ZnPc(Lys)_5$ is used in the following experiments.

2.2. Synthesis and Purification of $ZnPc(Lys)_5$

The asymmetric CPZ was prepared through statistical condensation of trimellitic anhydride and phthalic anhydride, at a ratio of 1:7, in the presence of urea, zinc acetate, and ammonium molybdate (Figure 1). Through a lengthy and laborious purification process, CPZ was obtained. The CPZ was then dissolved in 5% pyridine-containing N, N′-dimethylformamide. After carboxyl activation, pentalysine resin was added to initiate conjugation. The peptide C-termini of the pentalysine resin was attached to the resin and the peptide side chain was while the N-termini should be exposed. After the reaction, the $ZnPc(Lys)_5$ was cleaved from the resin using trifluoacetic acid, and subjected to reverse-phase chromatography and lyophilization, to obtain a product with a purity of 95% (Figure 1) [13].

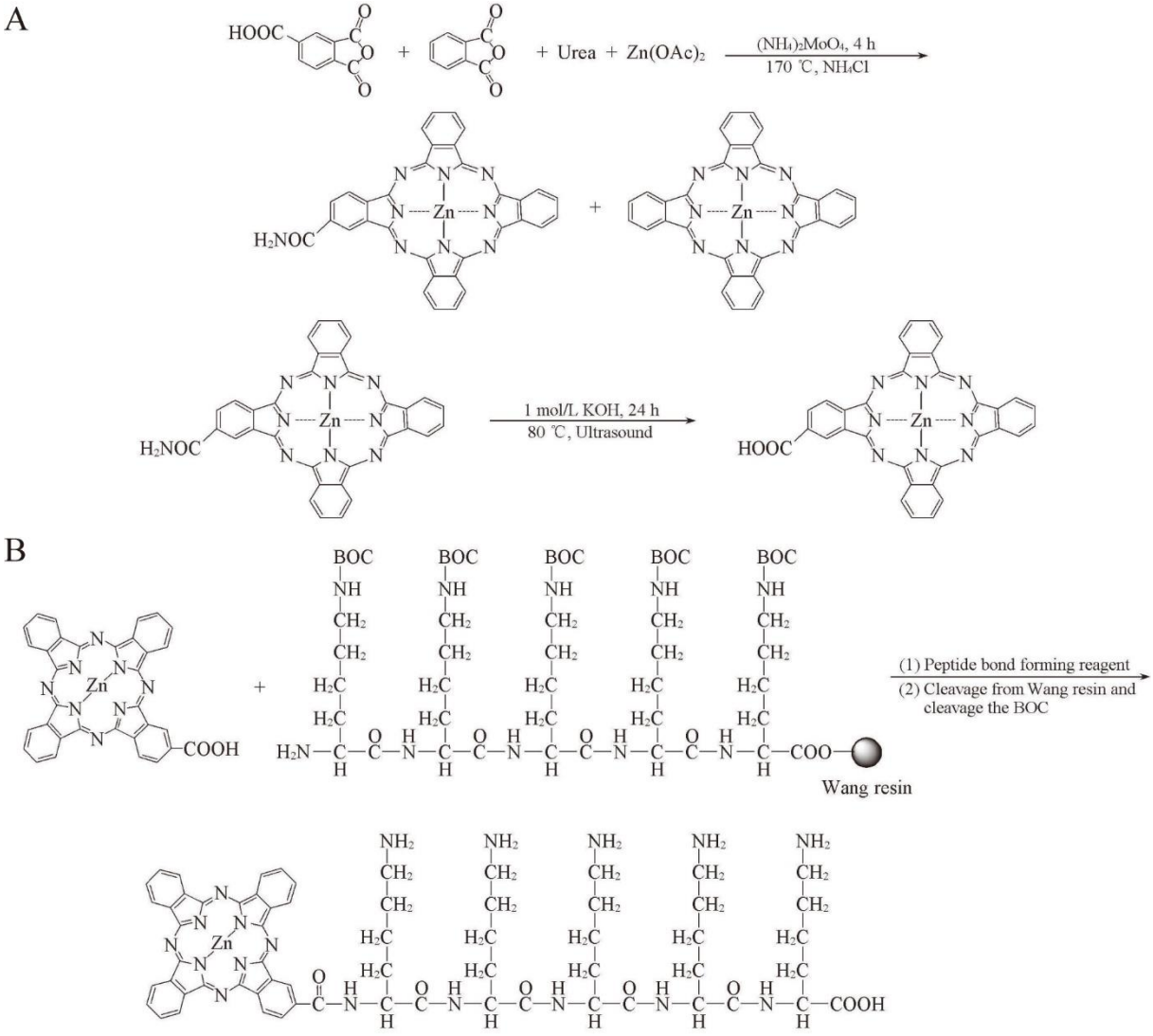

Figure 1. Synthesis of $ZnPc(Lys)_5$ [13]. (**A**) Synthesis of CPZ. (**B**) Synthesis of $ZnPc(Lys)_5$ by conjugating a pentalysine to CPZ.

2.3. Structural Characterization of ZnPc(Lys)$_5$

Chemical formula of ZnPc(Lys)$_5$ is $C_{63}H_{76}N_{18}O_7Zn$, with a theoretical molecular weight of 1262.8 Da. Mass spectrometry in methanol showed peaks at *m/z* 1263.90 ($[M+H]^+$) and *m/z* 632.5 ($[M+2H]^{2+}$); Infrared spectroscopy revealed characteristic peaks: a COOH stretching vibration at 1677.79 cm^{-1}, an N-C=O stretching vibration in the pentalysine chain at 1540.86 cm^{-1}, and a lysine side chain -$(CH_2)_4$- absorption peak at 723.18 cm^{-1} in the fingerprint region [13]. Two-dimensional proton NMR (Figure S1) confirmed all proton signals, with integration areas matching theoretical values, validating molecular structure of ZnPc(Lys)$_5$.

2.4. Chemical and Optical Properties of ZnPc(Lys)$_5$

Phthalocyanine photosensitizers exist in monomeric and aggregated forms. These forms of ZnPc(Lys)$_5$ can be identified using UV-Vis absorption or fluorescence spectroscopy. The absorption peak around 630 nm corresponds to aggregated conformer, while the peak around 675 nm corresponds to monomeric molecules. With an excitation wavelength of 610–630 nm, the monomer emits fluorescence around 690 nm, while aggregated molecules exhibiting little or no fluorescence, providing another way to identify its conformation. Generally, ZnPc(Lys)$_5$ is soluble in aqueous solution, but exists mainly as aggregates. However, in organic solvents like DMSO or in the presence of strong detergent (0.1 M NaOH + 1% SDS, typically used to lyse cells) ZnPc(Lys)$_5$ is predominantly monomeric. In DMSO, the maximum absorption wavelength of ZnPc(Lys)$_5$ is 678 nm, with a molar extinction coefficient of 118,380 L/(mol·cm) [13]. Monomeric ZnPc(Lys)$_5$, but not its aggregate form, generates singlet oxygen under light illumination, with a quantum yield of 0.64 (using unsubstituted zinc phthalocyanine as a standard and DPBF for singlet oxygen capture). Its solubility in aqueous solutions is 48–56 mM (60–70 g/L), predominantly in aggregates. Notably, aggregated ZnPc(Lys)$_5$ does not produce singlet oxygen, nor fluorescence, and at the same time, becomes more resistance to photodegradation, thus offering excellent stability [25]. These unique properties of ZnPc(Lys)$_5$ are key for its applications. Of note, ZnPc(Lys)$_5$ is positively charged in aqueous solution at neutral pH due to the high pKa value of lysine moiety.

3. Anti-Tumor Effects of ZnPc(Lys)$_5$

3.1. Cellular Experiments and Animal Studies

At a low light dose of 1.5 J/cm^2, ZnPc(Lys)$_5$ exerted strong killing effects on human hepatocellular carcinoma cells (Bel7402 IC_{50} = 1.95 μM), human gastric cancer cells (BGC823 IC_{50} = 3.05 μM), and human leukemia cells (K562 IC_{50} = 0.34 μM), when compared to normal embryonic fibroblast cells (HELF IC_{50} = 11.27 μM) [13]. This indicates that ZnPc(Lys)$_5$ achieves efficient targeting specificity towards cancer cells.

In the in vivo anti-tumor studies of ZnPc(Lys)$_5$, S180 mouse sarcoma cells were inoculated into the right axillary region of Kunming strain mice to establish an S180 tumor model. At a light dose of 65 J/cm^2, ZnPc(Lys)$_5$ inhibited tumor growth in a dose dependent manner, approaching its maximum tumor inhibition effect at 1 mg/kg (0.5 mg/kg, 61.4%; 1 mg/kg, 86.8%; 2 mg/kg, 84.4%)[20].

3.2. Pharmacokinetic Study of ZnPc(Lys)$_5$

After administering 2 mg/kg of ZnPc(Lys)$_5$ via tail vein injection into tumor-bearing mice, the amount of ZnPc(Lys)$_5$ in plasma and tissues was quantitatively analyzed using fluorescence spectrometry to evaluate its pharmacokinetic parameters and distribution[20]. The results showed that the total concentration of ZnPc(Lys)$_5$ in plasma decreased in a single-phase exponential manner over time, with a plasma elimination rate constant of 1.12 h^{-1} and a half-life of 0.6 h (Figure 2A). Following a single dose, ZnPc(Lys)$_5$ was widely distributed among various tissues, with the lowest concentration consistently observed in the brain (<500 ng/g), indicating that ZnPc(Lys)$_5$ does not readily cross the blood-brain barrier. The retention in the skin and muscle was low, and the ratio of ZnPc(Lys)$_5$ content in the tumor to that in the skin consistent at 2–4:1, suggesting continuous accumulation of ZnPc(Lys)$_5$ in the tumor (Figure 2B). The content of ZnPc(Lys)$_5$ in the liver was significantly higher than in other tissues (Figure 2C), which is attributed to the liver being the primary metabolic organ for ZnPc(Lys)$_5$ [25].

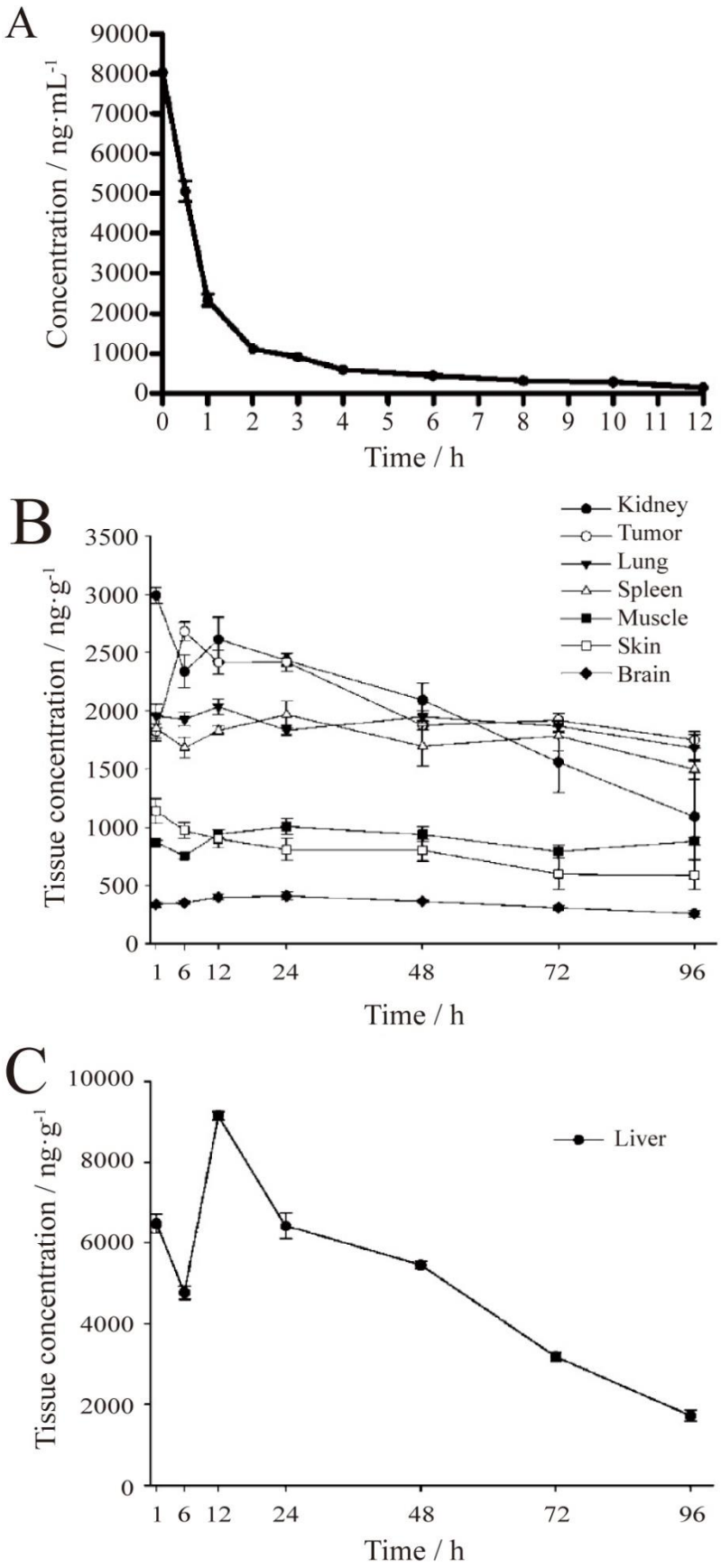

Figure 2. Biodistribution studies of ZnPc $(Lys)_5$ in S180 tumor-bearing mice [20]. (**A**) Plasma concentration of ZnPc$(Lys)_5$ (2 mg/kg, i.v.) as a function of time in S180 tumor-bearing mice; (**B**,**C**) Tissue concentrations (mean ± SEM) of ZnPc$(Lys)_5$ as a function of time after (2 mg/kg, i.v.) in S180 tumor-bearing mice (n = 5).

3.3. Toxicological Studies of ZnPc(Lys)$_5$

The toxicological safety of ZnPc(Lys)$_5$ was rigorously examined through various aspects, including the determination of its median lethal dose (LD_{50}), assessment of skin irritation, eye irritation, allergic reactions, and evaluation of its potential to induce chromosomal damage [26]. In an acute oral toxicity study conducted on Kunming strain mice, varying concentrations of ZnPc(Lys)$_5$ were administered as a single oral gavage with 0.2 mL per 10 g body weight to fasted mice. Throughout the 14-day observation period, all mice exhibited normal food and water consumption, good growth, and no overt signs of toxicity. Gross anatomical examination at the end of the study also revealed no apparent abnormalities. The results indicated that the acute oral LD_{50} of ZnPc(Lys)$_5$ exceeded 5000 mg/kg body weight, classifying it as practically non-toxic. Additionally, acute skin irritation and acute eye irritation tests performed on rabbits did not reveal any abnormal irritation symptoms.

In the skin sensitization test [26], 48 healthy, albino guinea pigs with intact skin were randomly divided into a test group, a negative control group, and a positive control group. Following challenge with the ZnPc(Lys)$_5$, 3 animals in the test group developed erythema on their skin, resulting in a sensitization rate of 18.75%. Thus, this skin sensitization test showed that ZnPc(Lys)5 was a mild sensitizer. Furthermore, in the mouse bone marrow polychromatic erythrocyte micronucleus test, ZnPc(Lys)$_5$ did not cause an increase in the micronucleus frequency of polychromatic erythrocytes in mouse bone marrow, indicating that it does not possess chromosomal damaging effects.

These findings suggest that ZnPc(Lys)$_5$ is a non-toxic, non-irritating, and mildly sensitizing substance.

3.4. Localization and Mechanism of Action of ZnPc(Lys)$_5$ within Cancer Cells

The singlet oxygen generated by the photodynamic effect has a lifetime in the nanosecond range, and a free diffusion distance, before quenched, of nanometer and up to 1 micrometer, thus limiting the damage to the organelle where the photosensitizer resides, leading to distinct cell death mechanisms. There are three primary mechanisms of cell death induced by photodamage [1]: (1) apoptosis, primarily caused by photosensitizers localized in mitochondria; (2) necrosis, more commonly observed with photodamage on the plasma membrane; (3) autophagocytosis, most likely triggered by photosensitizer targeting lysosomes. Consequently, analyzing the intracellular localization of photosensitizers becomes crucial in exploring their cell-killing mechanisms.

Fluorescence confocal microscopy experiments showed that ZnPc(Lys)$_3$ and ZnPc(Lys)$_9$ were primarily located in the cytoplasm of BGC823 cells, with the highest likelihood of being present in lysosomes and mitochondria [21]. Of note, ZnPc(Lys)$_5$ does not significantly accumulate in the cell nucleus. This avoids the potential for ZnPc(Lys)$_5$ to cause DNA mutations or saturate genomic repair capabilities, which could lead to instability in the genome of normal cells.

4. Antibacterial Effect of ZnPc(Lys)$_5$

4.1. Application in the Treatment of Periodontal Diseases

We have studied the antibacterial effect of ZnPc(Lys)$_5$ against *Porphyromonas gingivalis*, the primary pathogen responsible for oral gingivitis [17]. The results show that the uptake of ZnPc(Lys)$_5$ by *Porphyromonas gingivalis* exhibits a dose-dependent and time-dependent pattern. Compared to neutral or negatively charged phthalocyanine photosensitizers, ZnPc(Lys)$_5$ demonstrates higher uptake and faster absorption rates, owing to its positive charge that enhances binding to the strongly negatively charged bacterial outer membrane. In in vitro antibacterial studies, ZnPc(Lys)$_5$ potently inhibits the growth of *Porphyromonas gingivalis* in a light dose-dependent and photosensitizer concentration-dependent manner, while exhibiting no significant toxicity towards human periodontal ligament cells, indicating its selectivity towards bacteria.

Furthermore, a periodontitis model was established in beagle dogs, and antimicrobial experiments revealed that the similar ZnPc(Lys)$_n$ (phthalocyanine zinc conjugated with polylysine) photosensitizer effectively reduced the bacterial load inside the periodontal pockets by 100-fold [27], suggesting the potential of this photosensitizer for the treatment of periodontitis.

4.2. Application in the Treatment of Bacterial Skin Infections

Staphylococcus aureus and *Propionibacterium acnes* are primary causative agents of various skin infections, such as cellulitis, abscesses, and post-surgical infections. In in vitro antibacterial experiments, the survival rates of *Staphylococcus aureus* and *Propionibacterium acnes* were reduced by 4 log10 colony-forming units (CFUs) and 5–6 log10 CFUs, respectively, following PDT treatment (ZnPc(Lys)$_5$ at 1 μM concentration and light dose of

6 J/cm^2). In in vivo study on locally infected skin wounds in animal models, we inoculated bioluminescent *Staphylococcus aureus* into superficial excision wounds on the backs of rats. Following PDT treatment (ZnPc(Lys)$_5$ at 1 μM concentration and light dose of 15 J/cm^2), we observed and recorded the wound healing process for 12 consecutive days. The results showed that ZnPc(Lys)$_5$ treatment significantly accelerated wound healing. Using a laser speckle imaging system to assess the subcutaneous blood flow velocity at the wound site after complete healing (day 14), we found that the subcutaneous blood flow in wounds treated with ZnPc(Lys)$_5$ was close (only 1.4 fold higher, Figure 3C) to that of normal skin, whereas the ratio was 2.8 fold higher in wounds treated with a non-antibacterial agent ([ZnPc(SO$_3$)$_4$)]$^{8-}$, Figure 3) [28]. Thus, these findings indicate that ZnPc(Lys)$_5$ effectively eradicates pathogens, reduces inflammation in the skin wound area, and promotes wound healing, demonstrating its potential as an effective photosensitizer for treating bacterial skin infections.

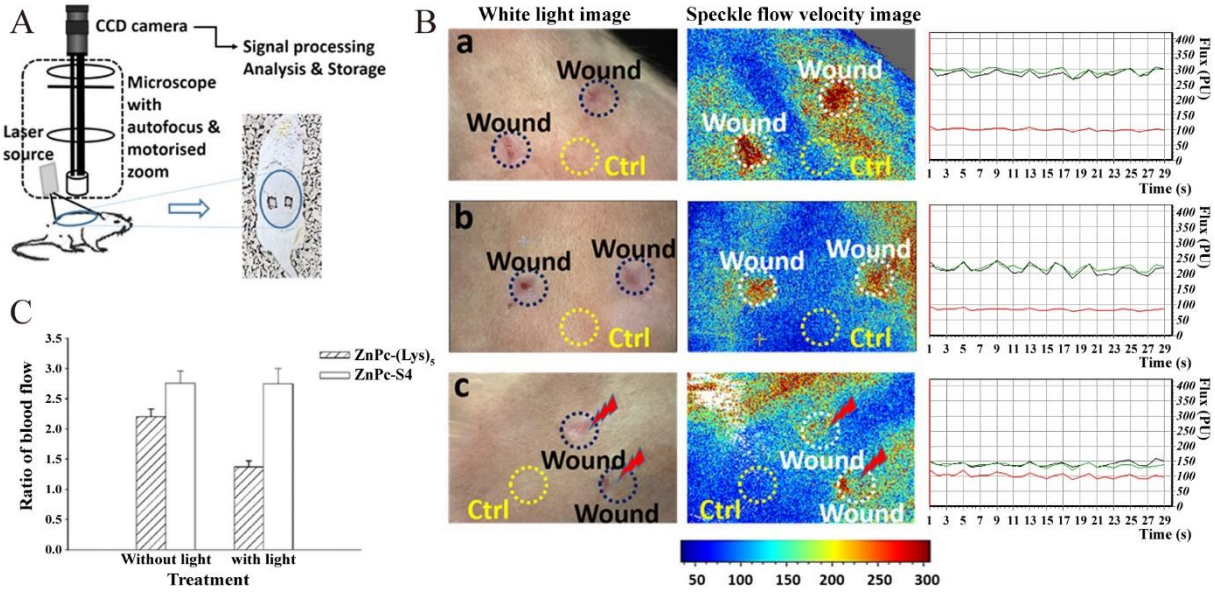

Figure 3. In vivo speckle imaging of *S. aureus* infected excisional wounds with rats treated with ZnPc(Lys)$_5$ or ZnPc-S4 [28]. (**A**) Schematic diagram of the laser speckle imaging system; (**B**) Three representative speckle images of the wound-skin rats treated with ZnPc-S4 (**a**) or ZnPc (Lys)$_5$ with (**c**) or without (**b**) irradiation (680 nm, 15 J/cm^2); (**C**) Analysis of the blood flow ratio under wound-skin of rats 2 weeks after treated with ZnPc(Lys)$_5$ or ZnPc-S4.

4.3. Application in Combating Multidrug-Resistant Bacteria

Based on the promising outcomes of ZnPc(Lys)$_5$ in treating bacterial periodontal and skin infections, we investigated its antibacterial activity against multidrug-resistant (MDR) bacteria, focusing on hospital-acquired MDR strains such as MDR *Escherichia coli* and MDR *Acinetobacter baumannii* [29]. Our results revealed that MDR *Escherichia coli* exhibited enhanced uptake of ZnPc(Lys)$_5$, and the growth of both MDR bacteria were significantly inhibited in a dose-dependent manner. Under light illumination at a dose of 12.75 J/cm^2, micromolar concentrations of ZnPc(Lys)$_5$ were sufficient to kill 6–6.5 log10 units of these MDR bacteria, with a stronger antibacterial effect observed against *Acinetobacter baumannii* compared to MDR *Escherichia coli*. Furthermore, we established local infections in mice by inoculating these two MDR bacteria into superficial excision wounds. Following a single session of PDT with ZnPc(Lys)$_5$, we observed effective inhibition of the growth of both MDR bacteria and accelerated wound healing.

So far, most PDT applications utilizing photosensitizer ZnPc(Lys)$_5$ involve localized infections, but their use in systemic infections is limited. PDT, however, offers several advantages over traditional antibiotics. It is widely recognized that PDT exhibits potent and broad-spectrum antibacterial activity and, more importantly, low resistance potential by pathogen [30].

4.4. Research on Antibacterial Mechanism of ZnPc(Lys)$_5$

4.4.1. Damage to cells by ROS

Through real-time fluorescent quantitative PCR, we measured the transcription level of anti-oxidative gene *sodA* and *oxyR* in *Escherichia coli* after exposure to photodynamic treatment with varying concentrations of ZnPc(Lys)$_5$[25]. The results showed that their transcription levels increased with the concentration of ZnPc(Lys)$_5$. When the concentration of ZnPc(Lys)$_5$ was set at 1/8, 1/4, and 1/2 of its MIC (minimum inhibitory concentration), respectively, the transcription level of *sodA* was upregulated by 5-fold, 16 fold, and 64 fold, while the *oxyR* level was upregulated by 11-fold, 64-fold, and 128-fold. These results indicated that bacteria produced anti-oxidation defense mechanisms to protect themselves against the ROS pressure generated by PDT before its defense mechanism is saturated by ROS at the MIC level of ZnPc(Lys)$_5$.

4.4.2. Damage to Bacterial DNA

Photodynamic therapy is typically believed to kill host cells by damaging their phospholipid bilayers, leading to the leakage of cellular contents or inactivation of membrane transport systems and enzymes on the phospholipid bilayer [31,32]. Given that ZnPc(Lys)$_5$ contains positively charged lysine residues, it is likely to target and disrupt the DNA in bacteria. Conversely, bacteria can initiate DNA repair via the SOS response, which involves upregulation of the *recA* gene to facilitate DNA repair and downregulation of the *lexA* gene, thereby lifting the inhibition of the SOS response. To study this hypothesis, we measured the transcription level of *recA* and *lexA* in *Escherichia coli* after its exposure to varying concentrations of ZnPc(Lys)$_5$ [25]. Our results showed that when the concentration of ZnPc(Lys)$_5$ was 1/8, 1/4, and 1/2 of its MIC, there were significant changes in the expression of *recA* (upregulated by 0.5, 2.5, and 4 times, respectively) and *lexA* (downregulated by 3, 11, and 16 times, respectively), indicating that the photodynamic antibacterial effect damaged the DNA, and the gene repair process indeed initiated. This result contrasts sharply with the situation in tumor cells, where ZnPc(Lys)$_5$ typically accumulate in the plasma membrane or the cytosol (typically mitochondria or lysosome), but NOT inside the cell nucleus, thus cannot damage the DNA on the mammalian cells.

5. The Efficacy of ZnPc(Lys)$_5$ against SARS-CoV-2

The severe acute respiratory syndrome coronavirus 2 (SARS-CoV-2) is the primary pathogen responsible for the novel coronavirus disease (COVID-19). Since its report in 2019, it has become a global pandemic, posing a significant threat to world public health. Currently, there is no preventive method specifically targeting SARS-CoV-2 infection [33]. We have reported the use of ZnPc(Lys)$_5$ in the prevention and treatment of COVID-19 [34].

The entry of SARS-CoV-2 into host cells is mediated by a host receptor, angiotensin-converting enzyme 2 (ACE2). Our results demonstrate that ZnPc(Lys)$_5$, under LED light illumination with a low light dose of 0.48 J/cm^2, exhibits excellent virus inactivation with an EC_{50} of 60.2 nM or EC_{90} at 331 nM. At a concentration of 1.0 μM, ZnPc(Lys)$_5$ completely eliminates SARS-CoV-2 load inside the host cells, and importantly, maintains the cell integrity as shown by the cell morphology, making it the most effective photosensitizer among those screened. The positive charges on ZnPc(Lys)$_5$ is an important feature attributing to this specificity based on the structure-functional studies of a series of photosensitizers with different chemical structures.

Taking into account that photodynamic antiviral therapy is primarily utilized as a localized treatment, and given that SARS-CoV-2 enters the body through the oral and nasal mucosa to cause infection, it is conceivable to consider administering ZnPc(Lys)$_5$ in the form of a spray into the mouth and nasal cavity. By exposing these areas to light, the virus can be inactivated, thereby achieving the effects of prevention and controlling its transmission.

6. Other Applications of ZnPc(Lys)$_5$

6.1. Fluorescent Probe for Both Diagnosis and PDT

Imaging pathological foci may improve early diagnosis and subsequent treatment of various diseases. The maximum absorption (λ = 675 nm) and emission (λ = 690 nm) of ZnPc(Lys)$_5$ in the near-infrared region enable it to achieve relatively high penetration depth (up to 0.5–1 cm) in biological tissues. Combined with its excellent fluorescence quantum yield, ZnPc(Lys)$_5$ can be a highly sensitive optical probe for imaging in biological tissues.

A photosensitizer-paclitaxel nano diagnostic therapy that integrates tumor imaging, chemotherapy, and PDT was designed in this paper [35]. This therapy leveraged the hydrophobic interaction and π-π stacking between ZnPc(Lys)$_5$ and paclitaxel to form nanoparticles. By utilizing fluorescence molecular tomograph (FMT), we

measured the drug distribution of nanoparticles at tumor sites and various organs in mice, and also demonstrate the potent in vivo anti-tumor effect.

Furthermore, we have successfully applied $ZnPc(Lys)_5$ to the imaging of blood clots in vivo [36]. We found that $ZnPc(Lys)_5$, at a concentration of 180 nM, binds tightly to blood clots formed in vitro. Structure-function studies using two different probes have demonstrated that such a strong binding is due to the complementarity between the $ZnPc(Lys)_5$ structure and the dual properties of blood clot, consisting fibrin and several cellular components such as red blood cells and platelets, inducing hydrophobicity associated with the aggregated fibrin, and the highly electronegative surface ascribed to the low isoelectric point (pI) of fibrin at ~6.0. Next, we established two mouse models of thromboembolism, namely pulmonary embolism and ischemic stroke, and successfully achieved real-time in vivo imaging of blood clots using $ZnPc(Lys)_5$. This study on real-time thrombus imaging promotes our research on another area—the development of novel thrombolytic drugs. Moreover, the thrombus targeting principle developed in this study also applies to other imaging modalities.

6.2. Stabilizers for Slowing Down the Photodegradation of Antibacterial Agents

The application of PDT in agriculture requires a cost-effective light source capable of large-area irradiation, making sunlight the prime choice. Organic dye BODIPY derivative DIBDP boasts a maximum absorption wavelength of approximately 540 nm, aligning well with the peak radiation wavelength of sunlight (520 nm). Citrus canker is a disease caused by pathogenic bacteria (*Xanthomonas citri* subsp. *Citri*) and primarily affects the leaves, branches, and fruits of citrus plants, thereby compromising fruit quality and yield. DIBDP exhibits excellent photophysical properties and effectively inactivates *Xanthomonas citri* subsp. *citri* (IC_{50} = 0.26 μM). However, DIBDP undergoes rapid photodegradation in solution upon exposure to sunlight. On the other hand, while $ZnPc(Lys)_5$ possesses robust antibacterial properties and photostability, its maximum absorption wavelength (675 nm) significantly deviates from the peak radiation wavelength of sunlight (520 nm). We have discovered that by mixing DIBDP and $ZnPc(Lys)_5$ in a molar ratio of 1:2 using DMSO as the solvent to form a photosensitizer complex, the stability of DIBDP is significantly enhanced (with a 15-fold reduced photodegradation rate). This method is simple, and the resultant complex exhibits far superior antibacterial activity compared to traditional copper-based bactericides [37].

6.3. Tooth Bleach

The dietary and lifestyle habits can influence the occurrence of tooth discoloration and yellowing. Tooth whitening has recently attracted significant attention due to increased demand. Tooth bleaching, as one of the means of tooth whitening, involves the use of chemical substances to remove endogenous or exogenous discoloration of natural teeth [38]. Commonly used bleaching agents for tooth whitening include hydrogen peroxide, carbamide peroxide, and sodium perborate. However, these bleaching agents may cause some side effects such as changes in the surface morphology of tooth enamel and degradation of collagen inside dentin.

We use $ZnPc(Lys)_5$ as the component for tooth whitening in enamel [39] or dentin [40]. $ZnPc(Lys)_5$ is odorless itself in an aqueous solution, and at working concentration, the compound appears pale bluish. We demonstrate that $ZnPc(Lys)_5$ significantly increases the whiteness of the teeth compared to the hydrogen peroxide, and no color reversion is noticed within one month after the bleaching procedure, demonstrating the stable bleaching capability of $ZnPc(Lys)_5$. Additionally, the effects of $ZnPc(Lys)_5$ on the surface morphology and structure of tooth enamel were evaluated through surface hardness tests, surface roughness tests, and scanning electron microscope observations. The results indicated that $ZnPc(Lys)_5$ did not significantly impact tooth enamel. Importantly, $ZnPc(Lys)_5$ does not break down the collagen inside dentin, in contrast to hydrogen peroxide, which degrades dentin collagen. Consequently, $ZnPc(Lys)_5$ holds strong potential in the field of tooth whitening.

7. The Effect of Aggregation of Photosensitizer on Its Photodynamic Efficacy

Although the introduction of pentalysine endowed $ZnPc(Lys)_5$ with high water solubility, the UV-Vis spectrum of $ZnPc(Lys)_5$ in PBS (pH = 7.4) indicated that $ZnPc(Lys)_5$ existed as a soluble aggregate (Figure 4A) [13]. Consistently, no significant photobleaching of $ZnPc(Lys)_5$ was observed in aqueous solution [41]. Interestingly, in the presence of suspension cells (K562), $ZnPc(Lys)_5$ aggregate partially dissociates and monomeric $ZnPc(Lys)_5$ is observed (Figure 4B) [13]. Such disintegration of $ZnPc(Lys)_5$ aggregate is also observed in the presence of adherent cells (BGC823), and a significant amount of $ZnPc(Lys)_5$ monomer is observed on the cell surface (Figure 4C,D) [21]. Such $ZnPc(Lys)_5$ aggregate to monomer conversion is also observed with bacteria, and, surprisingly, LED light illumination appears to promote this conversion [41]. Therefore, we conclude that $ZnPc(Lys)_5$ remains to be soluble aggregate in aqueous solution. Such aggregation state makes the photosensitizer

resistant to photobleaching. Thus, the photosensitizer aggregation is not always a negative event. The interaction of the biological membranes with ZnPc(Lys)$_5$ triggers the dissociation of the aggregate into monomer, whic is photodynamically active. This dynamic equilibrium between monomer and aggregate of photosensitizer is clearly presented in the case of ZnPc(Lys)$_5$, and is previously under-appreciated in PDT literature.

We hypothesize that (1) the phospholipid bilayer of the cell membrane facilitates the dissociation of ZnPc(Lys)$_5$ aggregate; (2) upon entering the cytosol, the monomer may re-aggregate, but upon interaction with organelles such as mitochondria or lysosomes, it likely dissociates back into monomers.

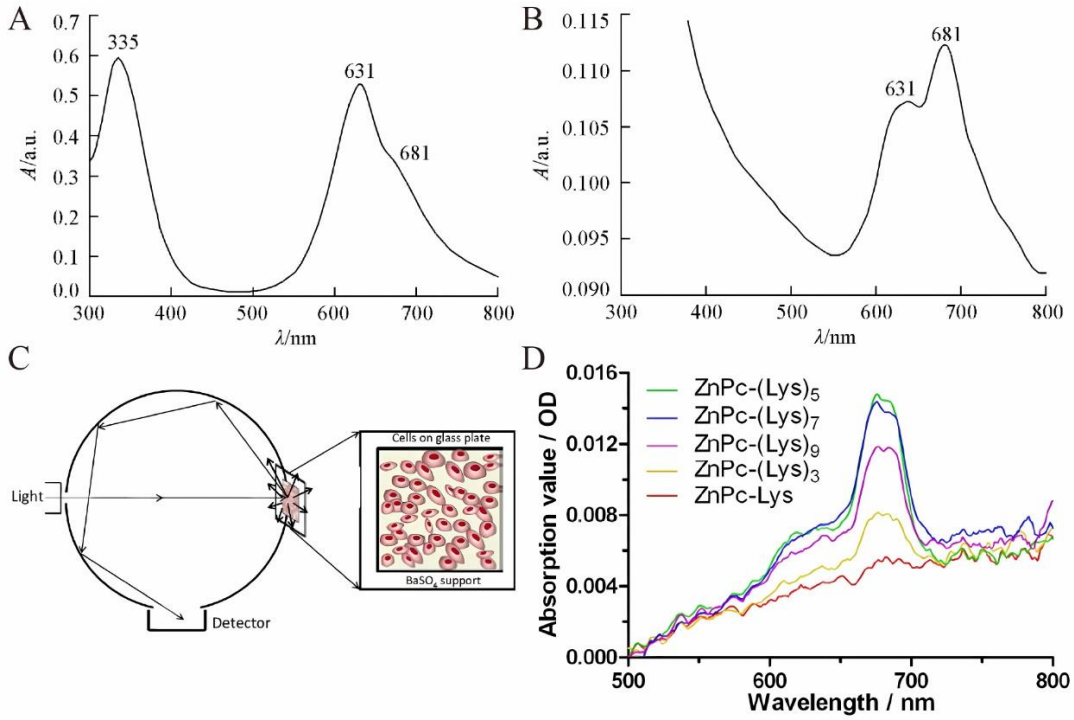

Figure 4. Ultraviolet-visible spectra of ZnPc (Lys)$_5$ under different conditions[13,21]. (**A**,**B**) UV-vis spectra of ZnPc(Lys)$_5$ in PBS (**A**) and in the presence of K562 cells (**B**); (**C**) Schematics of the diffusion reflectance measurement; (**D**) Diffusion reflectance spectra of ZnPc(Lys)n conjugates on BGC-823 cell surface.

Generally, the phthalocyanine aggregates can be classified into two cases: H-type (face-to-face stacks) and J-type (edge-to-edge contact). While the H-type aggregate is photodynamic inactive, and the J-aggregate can be photodynamic active [42]. Although there are some successful examples of exploring J-type aggregate for photodynamic, photothermal and/or photoacoustic applications[42], it is not completely clear how to generate J-type aggregate of phthalocyanine. In most cases, phthalocyanine aggregation is in H-type and does not show photodynamic activity.

On another hand, phthalocyanine derivatives can be designed and synthesized to make them completely water soluble and monomeric in aqueous solution. Such photosensitizer is not always preferred because the monomeric phthalocyanine is susceptible to photobleaching, potentially compromising its photodynamic efficiency. For example, we found that a ZnPc compound with its 12 periphery positions completely substituted with bulky and hydrophilic substituents (ZnPc(TAP)$_4^{12+}$) [43] is water soluble and completely monomeric, and shows good photodynamic effect. However, the compound is also rapidly photo-bleached during PDT.

8. Strategies for Promoting the Biomedical Applications of Phthalocyanines

At present, the photosensitizers used in clinical practice are porphyrins and phthalocyanines. Between these two classes, phthalocyanine absorbs light with longer wavelengths and has a higher absorption coefficient in the red/NIR region [12], but weak absorption at 400–600 nm [44], compared with porphyrins. Consequently, the skin phototoxicity in patients receiving phthalocyanine treatment is relatively low. Phthalocyanine photosensitizer has also higher photodynamic quantum yield, leading to much lower drug concentration needed for photodynamic treatment. Major challenges for the development of phthalocyanine-type photosensitizer are its low water solubility, poor tumor targeting, and unclear pharmacological kinetic behavior.

In this review, we demonstrate a simple but effective strategy to enable both the aqueous solubility and tumor targeting capability of phthalocyanine by coupling pentalysine moiety to phthalocyanine, giving to $ZnPc(Lys)_5$. On the other hand, based on our extensive works on phthalocyanine photosensitizers, we propose the aggregation of phthalocyanine as a critical factor in its photodynamic process. We showed that some degree of aggregation may improve stability of the photosensitizer during storage and delay its photobleaching during photodynamic treatment. Conversely, the aggregation of phthalocyanine should be reversible to ensure it can be effectively dispersed by cellular lipid bilayers and function as a monomer for photodynamic therapy.

9. Summary and Future Perspective

This work provides a comprehensive summary of research conducted by our team over the years on a novel photosensitizer, $ZnPc(Lys)_5$, which has enhanced water solubility and biological targeting capabilities through the incorporation of simple pentalysine as a functional module into phthalocyanine photosensitizer. $ZnPc(Lys)_5$ effectively and specifically eliminates tumor cells, multidrug-resistant bacteria, and SARS-CoV-2, exhibiting superior photodynamic effects while maintaining strong biosafety. Furthermore, $ZnPc(Lys)_5$ has great potential for applications beyond photodynamic therapy, such as serving as a probe and a tooth whitener, underscoring the versatile usage of photodynamic effect.

The results obtained during the development and applications of $ZnPc(Lys)_5$ suggests that a dynamic balance between monomeric and aggregate conformations is an important feature that improves the photodynamic effect and photostability of photosensitizers. Therefore, we propose that regulating photosensitizer aggregation should be a priority in the development of new photosensitizers for medical applications.

Supplementary Materials: The following supporting information can be downloaded at: URL, Figure S1: Two-dimensional nuclear magnetic resonance (NMR) spectrum of ZnPc(Lys)5.

Author Contributions: Z.C., J.C. (Jincan Chen), D.L., J.C. (Jingyi Chen), L.L., D.C., Z.C., P.X., L.J. completed partial research separately; N.C., J.H., and M.H. conceived and designed the study; Z.C., Y.C., Y.J., and M.H. wrote the manuscript. All authors have read and agreed to the published version of the manuscript.

Funding: This work was supported by the National Key R&D Project (2023YFE0118400), National Natural Science Foundation of China (32371312, 22077016, 82070142) and Natural Science Foundation of Fujian Province (2023Y4016, 2022J02017, 2021G02004, 2022J05175).

Data Availability Statement: Not applicable.

Conflicts of Interest: The authors declare no conflict of interest.

References

1. Van Straten, D.; Mashayekhi, V.; De Bruijn, H.; Oliveira, S.; Robinson, D. Oncologic Photodynamic Therapy: Basic Principles, Current Clinical Status and Future Directions. *Cancers* **2017**, *9*, 19. https://doi.org/10.3390/cancers9020019.
2. Agostinis, P.; Berg, K.; Cengel, K.A.; Foster, T.H.; Girotti, A.W.; Gollnick, S.O.; Hahn, S.M.; Hamblin, M.R.; Juzeniene, A.; Kessel, D.; et al. Photodynamic therapy of cancer: An update. *CA Cancer J. Clin.* **2011**, *61*, 250–281. https://doi.org/10.3322/caac.20114.
3. Li, X.S.; Lovell, J.F.; Yoon, J.; Chen, X.Y. Clinical development and potential of photothermal and photodynamic therapies for cancer. *Nat. Rev. Clin. Oncol.* **2020**, *17*, 657–674. https://doi.org/10.1038/s41571-020-0410-2.
4. Fenner, B.J.; Cheung, C.M.G.; Sim, S.S.; Lee, W.K.; Staurenghi, G.; Lai, T.Y.Y.; Ruamviboonsuk, P.; Kokame, G.; Yanagi, Y.; Teo, K.Y.C. Evolving treatment paradigms for PCV. *Eye* **2021**, *36*, 257–265. https://doi.org/10.1038/s41433-021-01688-7.
5. Ito, Y.; Ikeda, Y.; Iizuka, H. Cellulitis due to gas-producing organism with niveau formation. *J. Dermatol.* **2009**, *36*, 622–623. https://doi.org/10.1111/j.1346-8138.2009.00713.x.
6. Xiao, Q.; Mai, B.; Nie, Y.; Yuan, C.; Xiang, M.; Shi, Z.; Wu, J.; Leung, W.; Xu, C.; Yao, S.Q.; et al. In Vitro and In Vivo Demonstration of Ultraefficient and Broad-Spectrum Antibacterial Agents for Photodynamic Antibacterial Chemotherapy. *Acs Appl Mater Inter* **2021**, *13*, 11588–11596. https://doi.org/10.1021/acsami.0c20837.
7. Salmon-Divon, M.; Nitzan, Y.; Malik, Z. Mechanistic aspects of Escherichia coli photodynamic inactivation by cationic tetra-meso(N-methylpyridyl)porphine. *Photochem Photobiol Sci* **2004**, *3*, 423–429. https://doi.org/10.1039/b315627n.
8. Monro, S.; Colon, K.L.; Yin, H.; Roque, J., 3rd; Konda, P.; Gujar, S.; Thummel, R.P.; Lilge, L.; Cameron, C.G.; McFarland, S.A. Transition Metal Complexes and Photodynamic Therapy from a Tumor-Centered Approach: Challenges, Opportunities, and Highlights from the Development of TLD1433. *Chem Rev* **2018**, *119*, 797–828. https://doi.org/10.1021/acs.chemrev.8b00211.
9. Cai, L.Z.; Huang, M.D.; Chen, Z. Research progress of antitumor photosensitizers. *J. Fujian Med. Univ.* **2013**, 121–126. (In Chinese).

10. Josefsen, L.B.; Boyle, R.W. Photodynamic therapy: Novel third-generation photosensitizers one step closer? *Brit J Pharmacol* **2008**, *154*, 1–3. https://doi.org/10.1038/bjp.2008.98.
11. Alzeibak, R.; Mishchenko, T.A.; Shilyagina, N.Y.; Balalaeva, I.V.; Vedunova, M.V.; Krysko, D.V. Targeting immunogenic cancer cell death by photodynamic therapy: Past, present and future. *J. Immunother. Cancer* **2021**, *9*, e001926. https://doi.org/10.1136/jitc-2020-001926.
12. Galstyan, A. Turning Photons into Drugs: Phthalocyanine-Based Photosensitizers as Efficient Photoantimicrobials. *Chemistry* **2021**, *27*, 1903–1920. https://doi.org/10.1002/chem.202002703.
13. Chen, J.C.; Chen, H.W.; Li, Y.D.; Wang, J.D.; Chen, N.S.; Huang, J.L.; Huang, M.D. Preparation and Photodynamic activity of novel monosubstituted amphiphilic Zinc phthalocyanine. *Chem. J. China Univ.* **2008**, *29*, 2131–2137. https://doi.org/10.3321/j.issn:0251-0790.2008.11.003. (In Chinese).
14. Chen, D.; Song, M.R.; Huang, J.L.; Chen, N.S.; Xue, J.P.; Huang, M.D. Photocyanine: A novel and effective phthalocyanine-based photosensitizer for cancer treatment. *J. Innov. Opt. Health Sci.* **2020**, *13*, 2030009. https://doi.org/10.1142/S1793545820300098.
15. Chen, J.; Hou, L.; Zheng, K.; Wang, J.; Chen, N.; Huang, J.; Wu, M.; Xue, J. Blood distribution and plasma protein binding of PHOTOCYANINE: A promising phthalocyanine photosensitizer inphaseII clinical trials. *Eur. J. Pharm. Sci.Off. J. Eur. Fed. Pharm. Sci.* **2020**, *153*, 105491. https://doi.org/10.1016/j.ejps.2020.105491.
16. Chen, H.W.; Chen, J.C.; Chen, N.S.; Huang, J.L.; Wang, J.D.; Huang, M.D. Applications of Peptide Conjugated Photosensitizers in Photodynamic Therapy. *Prog. Biochem. Biophys.* **2010**, *36*, 1106–1113. https://doi.org/10.3724/sp.j.1206.2009.00080.
17. Chen, Z.; Zhou, S.Y.; Chen, J.C.; Li, L.S.; Hu, P.; Chen, S.; Huang, M.D. An effective zinc phthalocyanine derivative for photodynamic antimicrobial chemotherapy. *J. Lumin.* **2014**, *152*, 103–107. https://doi.org/10.1016/j.jlumin.2013.10.067.
18. Xiang, Y.L.; Tang, D.Y.; Yan, L.L.; Deng, L.L.; Wang, X.H.; Liu, X.Y.; Zhou, Q.H. Poly-l-lysine modified MOF nanoparticles with pH/ROS sensitive CIP release and CUR triggered photodynamic therapy against drug-resistant bacterial infection. *Int. J. Biol. Macromol.* **2024**, *266*, 131330. https://doi.org/10.1016/j.ijbiomac.2024.131330.
19. Chen, J.C.; Chen, N.S.; Huang, J.F.; Wang, J.D.; Huang, M.D. Derivatizable phthalocyanine with single carboxyl group: Synthesis and purification. *Inorg. Chem. Commun.* **2006**, *9*, 313–315.
20. Chen, Z.; Zhou, S.; Chen, J.; Deng, Y.; Luo, Z.; Chen, H.; Hamblin, M.R.; Huang, M. Pentalysine β-Carbonylphthalocyanine Zinc: An Effective Tumor-Targeting Photosensitizer for Photodynamic Therapy. *ChemMedChem* **2010**, *5*, 890–898. https://doi.org/10.1002/cmdc.201000042.
21. Li, L.S.; Luo, Z.P.; Chen, Z.; Chen, J.C.; Zhou, S.Y.; Xu, P.; Hu, P.; Wang, J.D.; Chen, N.S.; Huang, J.L.; et al. Enhanced Photodynamic Efficacy of Zinc Phthalocyanine by Conjugating to Heptalysine. *Bioconjugate Chem.* **2012**, *23*, 2168–2172.
22. Xu, P.; Chen, J.C.; Chen, Z.; Zhou, S.Y.; Hu, P.; Chen, X.Y.; Huang, M.D. Receptor-Targeting Phthalocyanine Photosensitizer for Improving Antitumor Photocytotoxicity. *PLoS ONE* **2012**, *7*, e37051. https://doi.org/10.1371/journal.pone.0037051.
23. Chen, Z.; Xu, P.; Chen, J.; Chen, H.; Hu, P.; Chen, X.; Lin, L.; Huang, Y.; Zheng, K.; Zhou, S.; et al. Zinc phthalocyanine conjugated with the amino-terminal fragment of urokinase for tumor-targeting photodynamic therapy. *Acta Biomater.* **2014**, *10*, 4257–4268. https://doi.org/10.1016/j.actbio.2014.06.026.
24. Lin, H.; Chen, J.; Zhang, Y.; Ulla, A.; Liu, J.; Lin, F.; Jiang, L.; Huang, M. Enhanced anti-microbial effect through cationization of a mono-triazatricyclodecane substituted asymmetric phthalocyanine. *J. Inorg. Biochem.* **2018**, *189*, 192–198. https://doi.org/10.1016/j.jinorgbio.2018.10.001.
25. Liu, D.F.; Li, L.S.; Chen, J.C.; Chen, Z.; Jiang, L.G.; Yuan, C.; Huang, M.D. Dissociation of zinc phthalocyanine aggregation on bacterial surface is key for photodynamic antimicrobial effect. *J. Porphyr. Phthalocyanines* **2018**, *22*, 925–934. https://doi.org/10.1142/S1088424618500888.
26. Cui, Y.; Wang, H.L.; Yin, F.; Xu, Z.; Qin, X.B.; Yu, K.N.; Cheng, P.P. Safety evaluation of amino acid photosensitive disinfectant. *J. Toxicol.* **2015**, *29*, 477–479. https://doi.org/10.16421/j.cnki.1002-3127.2015.06.021.
27. Chen, J.; Chen, Z.; Zheng, Y.; Zhou, S.; Wang, J.; Chen, N.; Huang, J.; Yan, F.; Huang, M. Substituted zinc phthalocyanine as an antimicrobial photosensitizer for periodontitis treatment. *J. Porphyr. Phthalocyanines* **2012**, *15*, 293–299. https://doi.org/10.1142/s1088424611003276.
28. Chen, Z.; Zhang, Y.X.; Wang, D.; Li, L.S.; Zhou, S.Y.; Huang, J.H.; Chen, J.C.; Hu, P.; Huang, M.D. Photodynamic antimicrobial chemotherapy using zinc phthalocyanine derivatives in treatment of bacterial skin infection. *J. Biomed. Opt.* **2016**, *21*, 018001. https://doi.org/10.1117/1.Jbo.21.1.018001.
29. Wang, D.; Zhang, Y.X.; Yan, S.F.; Chen, Z.H.; Deng, Y.C.; Xu, P.; Chen, J.C.; Liu, W.Z.; Hu, P.; Huang, M.D.; et al. An effective zinc phthalocyanine derivative against multidrug-resistant bacterial infection. *J. Porphyr. Phthalocyanines* **2017**, *21*, 205–210. https://doi.org/10.1142/S1088424617500298.
30. Wainwright, M.; Maisch, T.; Nonell, S.; Plaetzer, K.; Almeida, A.; Tegos, G.P.; Hamblin, M.R. Photoantimicrobials-are

we afraid of the light? *Lancet Infect. Dis.* **2017**, *17*, e49-e55. https://doi.org/10.1016/s1473-3099(16)30268-7.

31. Bertoloni, G.; Lauro, F.M.; Cortella, G.; Merchat, M. Photosensitizing activity of hematoporphyrin on Staphylococcus aureus cells. *Biochim. Biophys. Acta* **2000**, *1475*, 169–174. https://doi.org/10.1016/s0304-4165(00)00071-4.
32. Jori, G.; Fabris, C.; Soncin, M.; Ferro, S.; Coppellotti, O.; Dei, D.; Fantetti, L.; Chiti, G.; Roncucci, G. Photodynamic therapy in the treatment of microbial infections: Basic principles and perspective applications. *Lasers Surg. Med.* **2006**, *38*, 468–481. https://doi.org/10.1002/lsm.20361.
33. Xiling, G.; Yin, C.; Ling, W.; Xiaosong, W.; Jingjing, F.; Fang, L.; Xiaoyan, Z.; Yiyue, G.; Ying, C.; Lunbiao, C.; et al. In vitro inactivation of SARS-CoV-2 by commonly used disinfection products and methods. *Sci. Rep.* **2021**, *11*, 2418. https://doi.org/10.1038/s41598-021-82148-w.
34. Yu, S.J.; Sun, G.H.; Sui, Y.Q.; Li, H.L.; Mai, Y.H.; Wang, G.D.; Zhang, N.; Bi, Y.H.; Gao, G.F.; Xu, P.; et al. Potent inhibition of Severe Acute Respiratory Syndrome Coronavirus 2 by photosensitizers compounds. *Dye. Pigment.* **2021**, *194*, 109570. https://doi.org/10.1016/j.dyepig.2021.109570.
35. Li, L.L.; Chen, D.; Zheng, K.; Jiang, L.B.; Dai, T.; Yang, L.; Jiang, L.G.; Chen, Z.; Yuan, C.; Huang, M.D. Enhanced Antitumor Efficacy and Imaging Application of Photosensitizer-Formulated Paclitaxel. *ACS Appl. Mater. Interfaces* **2020**, *12*, 4221–4230. https://doi.org/10.1021/acsami.9b18396.
36. Chen, D.; Liu, P.W.; Liu, Y.R.; Wang, Z.Y.; Zhou, Y.; Jiang, L.G.; Yuan, C.; Li, Y.K.; Lin, W.; Huang, M.D. A Clot-Homing Near-Infrared Probe for In Vivo Imaging of Murine Thromboembolic Models. *Adv. Healthc. Mater.* **2022**, *11*, e2102213. https://doi.org/10.1002/adhm.202102213.
37. Jiang, L.B.; Liu, Y.R.; Xu, X.Y.; Su, D.; Zou, H.S.; Liu, J.Y.; Yuan, C.; Huang, M.D. Inhibition of the Citrus Canker Pathogen Using a Photosensitizer Assisted by Sunlight Irradiation. *Front. Microbiol.* **2020**, *11*, 571691. https://doi.org/10.3389/fmicb.2020.571691.
38. Li, Y.M. Stain removal and whitening by baking soda dentifrice A review of literature. *J. Am. Dent. Assoc.* **2017**, *148*, S20–S26. https://doi.org/10.1016/j.adaj.2017.09.006.
39. Li, Z.; Wu, Z.; Wang, J.; Huang, M.; Lin, M. Expanding the applications of photodynamic therapy—Tooth bleaching. *Clin. Oral Investig.* **2021**, *26*, 2175–2186. https://doi.org/10.1007/s00784-021-04199-7.
40. Wu, Z.; Wang, G.; Li, Z.; Li, Z.; Huang, D.; Huang, M.; Lin, M. Dental Bleaching with Phthalocyanine Photosensitizers: Effects on Dentin Color and Collagen Content. *Molecules* **2023**, *28*, 4223. https://doi.org/10.3390/molecules28104223.
41. Liu, D.; Jiang, L.; Chen, J.; Chen, Z.; Yuan, C.; Lin, D.; Huang, M. Monomer and Oligomer Transition of Zinc Phthalocyanine Is Key for Photobleaching in Photodynamic Therapy. *Molecules* **2023**, *28*, 4639. https://doi.org/10.3390/molecules28124639.
42. Bunin, D.A.; Martynov, A.G.; Gvozdev, D.A.; Gorbunova, Y.G. Phthalocyanine aggregates in the photodynamic therapy: Dogmas, controversies, and future prospects. *Biophys. Rev.* **2023**, *15*, 983–998. https://doi.org/10.1007/s12551-023-01129-7.
43. Zhang, Y.; Zheng, K.; Chen, Z.; Chen, J.; Hu, P.; Cai, L.; Iqbal, Z.; Huang, M. Rapid killing of bacteria by a new type of photosensitizer. *Appl. Microbiol. Biotechnol.* **2017**, *101*, 4691–4700. https://doi.org/10.1007/s00253-017-8133-8.
44. Chinna Ayya Swamy, P.; Sivaraman, G.; Priyanka, R.N.; Raja, S.O.; Ponnuvel, K.; Shanmugpriya, J.; Gulyani, A. Near Infrared (NIR) absorbing dyes as promising photosensitizer for photo dynamic therapy. *Coord. Chem. Rev.* **2020**, *411*, 213233. https://doi.org/10.1016/j.ccr.2020.213233.